

Gene Expression Profile and Signaling Pathways in MCF-7 Breast Cancer Cells Mediated by Acyl-CoA Synthetase 4 Overexpression

Ana F Castillo[#], Ulises D Orlando[#], Paula Lopez, Angela R Solano, Paula M. Maloberti and Ernesto J Podesta^{*}

Biomedical Research Institute, Inbiomed, Department of Biochemistry, School of Medicine University of Buenos Aires, CABA, C1121ABG, Argentina
[#]equally Contributed

Abstract

Aim: Breast cancer comprises a heterogeneous group of diseases that vary in morphology, biology, behavior and response to therapy. Previous studies have identified an acyl-CoA synthetase 4 (ACSL4) gene-expression pattern correlated with very aggressive tumors. In particular, we have used the tetracycline Tet-Off system to stably transfect non-aggressive breast cancer MCF-7 cells and developed a stable line overexpressing ACSL4 (MCF-7 Tet-Off/ACSL4). As a result, we have proven that cell transfection solely with ACSL4 cDNA renders a highly aggressive phenotype *in vitro* and results in the development of growing tumors when injected into nude mice. Nevertheless, and in spite of widespread consensus on the role of ACSL4 in mediating an aggressive phenotype in breast cancer, the early steps through which ACSL4 increases tumor growth and progression have been scarcely described and need further elucidation. For this reason, the goal of this work was to study the gene expression profile and the signaling pathways triggered by ACSL4 overexpression in the mechanism that leads to an aggressive phenotype in breast cancer.

Methods: We have performed a massive in-depth mRNA sequencing approach and a reverse-phase protein array using MCF-7 Tet-Off/ACSL4 cells as a model to identify gene expression and functional proteomic signatures specific to ACSL4 overexpression.

Results and Conclusion: The sole expression of ACSL4 displays a distinctive transcriptome and functional proteomic profile. Furthermore, gene networks most significantly upregulated in breast cancer cells overexpressing ACSL4 are associated to the regulation of embryonic and tissue development, cellular movement and DNA replication and repair. In conclusion, ACSL4 is an upstream regulator of tumorigenic pathways. Because an aggressive tumor phenotype appears in the early stages of metastatic progression, the previously unknown mediators of ACSL4 might become valuable prognostic tools or therapeutic targets in breast cancer.

Keywords: Acyl-CoA synthetase 4; Gene signature; Transcriptome; Functional proteomics; Breast cancer

Introduction

Breast cancer remains the second most important cause of death (by cancer) among women [1]. Patients who cannot be cured are those in whom breast cancer has metastasized, that is, breast cancer cells have migrated and invaded other organs such as lung and bone. As no effective therapies are currently available, aggressive breast cancer constitutes a key field for both researchers and clinicians. It has been shown that both in breast cancer cell lines and in tumor samples the expression of acyl-CoA synthetase 4 (ACSL4) is directly correlated with aggressiveness in breast cancer and inversely correlated with estrogen receptor alpha (ER α) levels [2-4]. ACSL4 belongs to a five-member family of enzymes that esterifies mainly arachidonic acid (AA) into acyl-CoA [2-5]. Unlike the other ACSL isoforms, ACSL4 is encoded on the X chromosome and its expression is highest in adrenal cortex, ovary and testis [6-10], as well as in mouse and human cerebellum and hippocampus [11]. Studies on the physiological functions of ACSL4 have revealed possible roles in polyunsaturated fatty acid metabolism in brain, in steroidogenesis, in eicosanoid metabolism related to apoptosis and embryogenesis [8-14]. ACSL4 expression has also been associated with non-physiological functions such as mental retardation disorder [15,16] and cancer [2,3,17,18]. ACSL4 was first associated with cancer due to its abnormal expression in colon and hepatocellular carcinoma. Increased ACSL4 expression, both at mRNA and protein levels [18], in colon adenocarcinoma cells has been associated with the inhibition of apoptosis and an increase in cell proliferation when compared to adjacent normal tissue. ACSL4 has also been suggested as a predictive factor for drug resistance in breast cancer patients receiving adriamycin-containing chemotherapy [19]. We have demonstrated a positive correlation of ACSL4 expression and aggressiveness in breast cancer cell lines, with the highest expression found in metastatic lines derived from triple-negative tumor breast cancer (MDA-MB-231 and Hs578T) [3]. Functionally, we have found

that ACSL4 is part of the mechanism responsible for increased breast cancer cell proliferation, invasion and migration, both *in vitro* and *in vivo* [3,4]. We have further demonstrated that ACSL4 can be silenced to reduce cell line aggressiveness. The role of ACSL4 in the development of growing tumors found further support when tumor growth was inhibited through the inhibition of ACSL4 expression [5]. However, even if the role of ACSL4 in mediating an aggressive phenotype in breast cancer is well accepted, its underlying mechanisms have been scarcely explored. For this reason, the goal of this work was to study the gene expression profile and the signaling pathways triggered by ACSL4 overexpression in the mechanism that leads to an aggressive phenotype in breast cancer. Thus, we have performed a massive in-depth mRNA sequencing approach and a reverse-phase protein array using ACSL4-overexpressing MCF-7 cells, as a model to identify gene expression and functional proteomic signatures specific to ACSL4 overexpression.

Materials and Methods

Cell culture

The human breast cancer cell line was generously provided by Dr.

***Corresponding author:** Ernesto J Podesta, Biomedical Research Institute, Inbiomed, Department of Biochemistry, School of Medicine University of Buenos Aires, CABA, C1121ABG, Argentina, Tel: 541149644027; E-mail: ernestopodesta@yahoo.com.ar

Received October 23, 2015; **Accepted** November 20, 2015; **Published** November 23, 2015

Citation: Castillo AF, Orlando UD, Lopez P, Solano AR, Maloberti PM, et al. (2015) Gene Expression Profile and Signaling Pathways in MCF-7 Breast Cancer Cells Mediated by Acyl-CoA Synthetase 4 Overexpression. Transcriptomics 3: 120. doi:10.4172/2329-8936.1000120

Copyright: © 2015 Castillo AF, et al. This is an open-access article distributed under the terms of the Creative Commons Attribution License, which permits unrestricted use, distribution, and reproduction in any medium, provided the original author and source are credited.

Vasilios Papadopoulos (Research Institute of the McGill University Health Centre, Montreal, Canada) and obtained from the Lombardi Comprehensive Cancer Center (Georgetown University Medical Center, Washington D.C., USA). The tetracycline-repressible MCF-7 cell lines, designated MCF-7 Tet-Off empty vector, and MCF-7 Tet-Off-induced repression of ACSL4, designated MCF-7 Tet-Off/ACSL4, were obtained previously in the laboratory [3]. The cell lines were maintained in Dulbecco's modified Eagle (DMEM) medium (GIBCO, Invitrogen Corporation, Grand Island, NY, USA) supplemented with 10% Fetal calf serum (PAA laboratories GmbH, Pasching, Austria) plus 100 U/ml penicillin and 10 mg/ml streptomycin (GIBCO, Invitrogen Corporation, Grand Island, NY, USA). Doxycycline (Sigma Chemical Co., St. Louis, MO, USA), a more stable tetracycline analogue, was used to regulate the expression of the Tet-Off system. Sterile and plastic material for tissue culture was from Orange Scientific (Braine-l'Alleud, Belgium). All other reagents were of the highest grade available.

RNA-Seq sample preparation and sequencing

For each cell line, total RNA was extracted by Direct-zol RNA kit (Zymo Research, Irvine, CA, USA). RNA quality was assessed by agarose gel electrophoresis (visual absence of significant 28S and 18S rRNA degradation) and by spectrophotometry. RNA-Seq was performed by Zymo Research facility performing PolyA enrichment of the RNA samples. HiSeq 2 x 50 bp paired-ends reads from RNA-Seq of a human normal-tumor pair samples were analyzed first using the TopHat and Cufflinks software. TopHat (v2.0.6) was utilized for alignment of short reads to GRCh37, Cufflinks (v2.0.2) for isoform assembly and quantification, and *commerbund* (v2.0.0) for visualization of differential analysis. Default parameters were used. The RNA-Seq quality control was performed using Dispersion, Volcano, MA, Density, PCA, Scatter and Box plots.

Quantitative reverse transcription-PCR (qRT-PCR)

MCF-7 Tet-Off empty vector and MCF-7 Tet-Off/ACSL4 total RNA was extracted using Tri-Reagent (Molecular Research Center, Cincinnati, OH, USA) following the manufacturer's instructions. Any residual genomic DNA was removed by treating RNA with DNase I (Invitrogen, Carlsbad, CA, USA) at room temperature for 15 min, which was subsequently inactivated by incubation with 2.5 mM EDTA for 10 min at 65°C. Two µg of total RNA were reverse transcribed using random hexamers and M-MLV Reverse Transcriptase (Promega, Madison, WI, USA) according to the manufacturer's protocol. For real-time PCR, gene specific primers were obtained from RealTimePrimers.com (Elkins Park, PA, USA). Real-time PCR was performed using Applied Biosystems 7300 Real-Time PCR System and 20 µl of a solution containing 5 µl of cDNA, 10 µM forward and reverse primers, and 10 µl of SYBR Select Master Mix (Applied Biosystems, Carlsbad, CA, USA) for each reaction. All reactions were performed in triplicate. Amplification was initiated by a 2-min preincubation at 50°C, 2-min incubation at 95°C, followed by 40 cycles at 95°C for 15 sec, 55°C for 15 sec and 72°C for 1 min, terminating at 95°C for the last 15 sec. Gene mRNA expression levels were normalized to human 18S RNA expression, performed in parallel as endogenous control. Real-time PCR data were analyzed by calculating the $2^{-\Delta\Delta Ct}$ value (comparative Ct method) for each experimental sample.

David and Ingenuity Pathways Analysis

To identify the statistically significant biological functions and signaling pathways affected by the genes differentially expressed in our comparisons, we used Database for Annotation, Visualization and Integrated Discovery (DAVID) [20] and Ingenuity Pathways Analysis

(IPA; Ingenuity Systems, Inc., Cambridge, MA, USA) [21]. IPA is the largest curated database and analysis system for understanding the signaling and metabolic pathways, molecular networks and biological processes that are most significantly changed in a dataset of interest. Ranking and significance of the biofunctions and the canonical pathways were tested by the *p*-value. Additionally, canonical pathways were ordered by the ratio (number of genes from the input data set that map to the pathway divided by the total number of molecules that exist in the canonical pathway). IPA also generated cellular networks where the differentially regulated genes were related according to previously known associations between genes or proteins, but independently of established canonical pathways. Top networks represent associative network functions based on a score that considers the $-\log(p\text{-value})$, which aggregates the likelihood that genes in the network are found together due to random chance.

Reverse phase protein assay (RPPA)

RPPA was performed in the RPPA Core Facility - Functional Proteomics from MD -Anderson Cancer Center, University of Texas, TX, USA. Cellular proteins were denatured by 1% SDS (with beta-mercaptoethanol) and diluted in five 2-fold serial dilutions in dilution buffer (lysis buffer containing 1% SDS). Serial diluted lysates were arrayed on nitrocellulose-coated slides (Grace Biolab) by Aushon 2470 Arrayer (Aushon BioSystems) [22].

Statistical Analysis

Data analysis was performed using GraphPad InStat Software 3.01 (La Jolla, CA, USA). Statistical significance was determined by analysis of variance (ANOVA) followed by Tukey-Kramer Multiple Comparison Test and Spearman's rank correlation coefficient was calculated using Social Science Statistics free statistics software.

Results and Discussion

Differential gene expression triggered by ACSL4

As ACSL4 plays a crucial role in tumor growth, we have undertaken a systematic study to identify genes with tumorigenesis capacity and elucidate the underlying signaling mechanism. Toward understanding the capacity of ACSL4 in the regulation of tumorigenesis, we have previously reported the involvement of AA lipoxygenase and cyclooxygenase metabolites in the action of ACSL4 [3,4] and, in this report, we focus on the identification of ACSL4-responsive genes using the RNA-Seq in MCF-7 Tet-Off/ACSL4 compared with an MCF-7 Tet-Off empty vector. This system is particularly valuable in enabling both the overexpression and the specific inhibition of ACSL4 through doxycycline treatment and has been previously used to develop tumors in xenograft models [3,4]. Results show a total of 26705366 RNA-Seq reads acquired from MCF-7 Tet-Off/ACSL4 and 22258811 reads acquired from MCF-7 Tet-Off empty vector. We next aligned the sequence reads to a human genome reference (GRCh37) using TopHat version 2.0.6, with results rendering 93.30% of the MCF-7 Tet-Off/ACSL4 reads and 92.90% of the MCF-7 Tet-Off empty vector reads as successfully mapped. The resulting read alignments (file format: BAM) were then assembled through Cufflinks version 2.0.2 for isoform assembly and quantification, and *commerbund* (v2.0.0) for visualization of differential analysis (default parameters were used). The RNA-Seq quality control was performed using Dispersion, Volcano, MA, Density, PCA, Scatter and Box plots. Gene expression levels were determined by measuring the sum of fragments per kilobase of exon model per million of reads mapped (FPKM), analyzed in each exon. To acquire more accurate results, data were filtered out whenever

estimated FPKM values in both MCF-7 Tet-Off/ACSL4 and MCF-7 Tet-Off empty vector samples were less than 1.0 (cf. an FPKM value of 0.05 is commonly set as the lowest boundary of expression level). Only loci having a \log_2 (fold change) > 2 between MCF-7 Tet-Off/ACSL4 and MCF-7 Tet-Off empty vector were considered. Ultimately, we observed that, from 32247 successfully sequenced loci, 3944 were significantly and differentially expressed in MCF-7 Tet-Off/ACSL4 samples. Among them, 2501 were upregulated and 1443 were downregulated. ACSL4 gene was one of the genes taken as a control of its overexpression and, as expected, it was one of the genes showing major differences between MCF-7 Tet-Off/ACSL4 and MCF-7 Tet-Off empty vector. Table 1 shows the top genes which exhibit differential changes when ACSL4 is overexpressed. To determine the characteristic chromosomal location of genes controlled by ACSL4 expression, we used the CROC program [23] to examine the expression landscape by plotting the number of differentially expressed genes along the whole chromosomes. Results revealed that chromosome distribution patterns varied greatly with respect to gene density and, in particular, chromosome 1 showed the highest gene density among genes mapped (Figure S1). A total of 52 clusters were found –chromosome 1 showed the highest number of clusters (8)-, while the number of genes in clusters was 181.

Enriched functional categories of gene networks relating to the transcripts regulated by ACSL4 overexpression

To gain insights into biological cell properties, IPA was used to rank enriched functional categories of gene networks relating to the transcripts regulated in ACSL4-responsive gene sets acquired from the RNA-Seq data. The highest-scoring associated diseases and disorders are shown in Table 2, while cancer was the disease showing the lowest *p*-value among diseases and disorders. As a result, we verified 390 top biofunctions concerned with the ACSL4-induced transcriptome alteration in MCF-7 Tet-Off/ACSL4 cells. The most significantly tumorigenesis-related biofunctions (only *p*-values under 0.01) are shown in Table 3. In agreement with our previous results regarding ACSL4 effect on cell proliferation, invasion and migration [3,4], the top three biofunctions which were IPA-predicted to be increased in RNA-Seq data were cell movement migration and proliferation. Table S1 shows a detailed list of molecules altered in these biofunctions. Table 4 shows the top ten most significantly upregulated functions related to gene networks in the RNA-Seq –along with a list of the corresponding genes in each function network–, while Figure S2 shows the network corresponding to the top ten upregulated functions. DNA replication,

GENES UPREGULATED				
Name	Gene Symbol	Location	Type(s)	log ₂ fold change
NADPH oxidase 3	<i>NOX3</i>	cytoplasm	enzyme	13.21
De-etiolated homolog 1 (Arabidopsis)	<i>DET1</i>	nucleus	other	10.97
Patched 2	<i>PTCH2</i>	plasma membrane	transmembrane receptor	10.9
Wingless-type MMTV integration site family, member 6	<i>WNT6</i>	extracellular space	other	6.74
Zinc finger, matrin-type 4	<i>ZMAT4</i>	nucleus	other	5.02
Retinoic acid induced 2	<i>RAI2</i>	unknown	other	4.75
Dual specificity phosphatase 18	<i>DUSP18</i>	cytoplasm	phosphatase	4.69
Transcription factor B1, mitochondrial	<i>TFB1M</i>	cytoplasm	transcription regulator	4.58
MAP/microtubule affinity-regulating kinase 1	<i>MARK1</i>	cytoplasm	kinase	4.30
Interleukin 20	<i>IL20</i>	extracellular space	cytokine	4.29
Fatty acyl CoA reductase 2	<i>FAR2</i>	cytoplasm	enzyme	4.16
Ets homologous factor	<i>EHF</i>	nucleus	transcription regulator	4.09
SH3-domain GRB2-like 3	<i>SH3GL3</i>	cytoplasm	other	4.06
2'-5'-oligoadenylate synthetase 1, 40/46kDa	<i>OAS1</i>	cytoplasm	enzyme	4.05
Synaptotagmin XIII	<i>SYT13</i>	plasma membrane	transporter	3.85
Aldehyde oxidase 1	<i>AOX1</i>	cytoplasm	enzyme	3.78
G protein, alpha inhibiting activity	<i>GNAI1</i>	plasma membrane	enzyme	3.78
FXRD domain containing ion transport regulator 5	<i>FXRD5</i>	plasma membrane	ion channel	3.75
Cytochrome c oxidase subunit VIIb2	<i>COX7B2</i>	unknown	unknown	3.73
Wingless-type MMTV integration site family, member 10A	<i>WNT10A</i>	extracellular space	other	3.60
Interferon, alpha-inducible protein 6	<i>IFI6</i>	cytoplasm	other	3.35
Sp6 transcription factor	<i>SP6</i>	nucleus	transcription regulator	3.35
Acyl-CoA oxidase 2, branched chain	<i>ACOX2</i>	cytoplasm	enzyme	3.31
Transforming growth factor, beta 2	<i>TGFB2</i>	extracellular space	growth factor	3.22
Interleukin 24	<i>IL24</i>	extracellular space	cytokine	3.15
GABA(A) receptor-associated protein like 1	<i>GABARAPL1</i>	cytoplasm	other	2.54
FBJ murine osteosarcoma viral oncogene homolog	<i>FOS</i>	nucleus	transcription regulator	2.41
Laminin, beta 1	<i>LAMB1</i>	extracellular space	other	2.37
Nuclear receptor coactivator 4	<i>NCOA4</i>	nucleus	transcription regulator	2.09
Phospholipase D1, phosphatidylcholine-specific	<i>PLD1</i>	cytoplasm	enzyme	2.09
v-Erb-b2	<i>ERBB2</i>	plasma membrane	kinase	2.05
Fibroblast growth factor 11	<i>FGF11</i>	extracellular space	other	2.04
Ret proto-oncogene	<i>RET</i>	plasma membrane	kinase	2.04
Fibroblast growth factor receptor 1	<i>FGFR1</i>	plasma membrane	kinase	2.04
Integrin, alpha 2 (CD49B, alpha 2 subunit of VLA-2 receptor)	<i>ITGA2</i>	plasma membrane	transmembrane receptor	2.02
Eukaryotic translation initiation factor 2-alpha kinase 2	<i>EIF2AK2</i>	cytoplasm	kinase	1.94
Unc-51 like autophagy activating kinase 1	<i>ULK1</i>	cytoplasm	kinase	1.83
Vascular endothelial growth factor A	<i>VEGFA</i>	extracellular space	group	1.75

GENES DOWNREGULATED				
Name	Gene Symbol	Location	Type(s)	log ₂ fold change
Protein tyrosine phosphatase, non-receptor type 22	<i>PTPN22</i>	cytoplasm	phosphatase	-11.55
ADAM metallopeptidase with thrombospondin type 1 motif, 9	<i>ADAMTS9</i>	extracellular space	peptidase	-11.21
Prickle homolog 2	<i>PRICKLE2</i>	nucleus	other	-11.08
Neurotrophic tyrosine kinase, receptor, type 3	<i>NTRK3</i>	plasma membrane	kinase	-8.13
Contactin associated protein-like 3B	<i>CNTNAP3B</i>	unknown	other	-7.29
WNT inhibitory factor 1	<i>WIF1</i>	extracellular space	other	-4.75
Keratin, Type I cytoskeletal 20	<i>CK20 (KRT20)</i>	cytoplasm	other	-4.22
Deiodinase, iodothyronine, type II	<i>DIO2</i>	cytoplasm	enzyme	-3.62
Zinc finger protein 217	<i>ZNF217</i>	nucleus	transcription regulator	-3.41
Ca ⁺⁺ -dependent secretion activator	<i>CADPS</i>	plasma membrane	other	-3.15

Table 1: Identification of significantly upregulated and downregulated genes by ACSL4 overexpression using RNA-Seq.

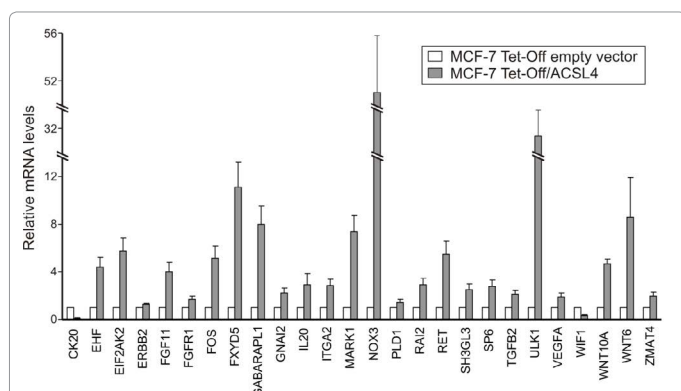


Figure 1: Real-time RT-PCR analysis of the top genes exhibiting differential changes in RNA-Seq when ACSL4 is overexpressed. Total RNA was isolated from MCF-7 Tet-Off empty vector and MCF-7 Tet-Off/ACSL4 cells, reverse transcribed and subjected to real-time PCR using specific primers. Each transcript expression level was normalized to human 18S RNA expression, performed in parallel as endogenous control. Real-time PCR data were analyzed by calculating the $2^{-\Delta\Delta Ct}$ value (comparative Ct method) for each experimental sample. Relative mRNA expression levels are shown. Data are presented as mean \pm standard deviation (SD).

Name of Diseases and Disorders	p-value	# molecules
Cancer	5.74E-07 - 0.0191	530
Infectious Disease	4.56E-05 - 0.0174	136
Reproductive System Disease	7.35E-05 - 1.87E-02	163
Dermatological Diseases and Conditions	8.42E-05 - 0.0141	74
Endocrine System Disorders	1.09E-04 - 0.0197	78

Table 2: Top associated diseases and disorders analyzed by IPA. Top significantly diseases and disorders concerned with the ACSL4-induced transcriptome alteration in MCF-7 Tet-Off/ACSL4 cells.

Category	Diseases or Functions Annotation	p-value	Predicted Activation State	Activation z-score	# Molecules
Cellular Movement	cell movement	3.97E-07	Increased	4.685	182
Cellular Movement	migration of cells	4.65E-07	Increased	4.677	166
Cellular Growth and Proliferation	proliferation of cells	2.04E-06	Increased	2.390	295
Cellular Assembly and Organization	formation of cellular protrusions	7.15E-05	Increased	3.830	73
Cellular Assembly and Organization	microtubule dynamics	1.48E-04	Increased	4.169	94
Cellular Assembly and Organization	organization of cytoskeleton	1.89E-04	Increased	3.662	107

Gene Expression	transactivation	3.17E-04	Increased	3.318	59
Cellular Assembly and Organization	organization of cytoplasm	3.73E-04	Increased	3.714	113
Carbohydrate Metabolism	sulfation of polysaccharide	4.39E-04	Increased	2.132	5
Gene Expression	transactivation of RNA	9.23E-04	Increased	3.718	54
Cancer	proliferation of cancer cells	1.05E-03	Increased	2.009	37
Cellular Assembly and Organization	formation of plasma membrane projections	1.20E-03	Increased	2.128	49
Cellular Growth and Proliferation	proliferation of connective tissue cells	1.45E-03	Increased	2.628	54
Cellular Development	branching of cells	1.60E-03	Increased	3.043	17
Cellular Movement	cell movement of tumor cell lines	2.20E-03	Increased	2.034	67
Cellular Movement	migration of tumor cell lines	2.26E-03	Increased	2.139	55
Cellular Movement	cell movement of tumor cells	2.41E-03	Increased	2.530	19
Cell Morphology	shape change of tumor cell lines	5.81E-03	Increased	2.180	16
Cellular Development	differentiation of stem cells	8.78E-03	Increased	2.540	21
Cancer	prostate cancer and tumors	1.17E-02	Increased	2.200	54
Cellular Assembly and Organization	growth of plasma membrane projections	1.18E-02	Increased	2.866	40
Cellular Movement	migration of tumor cells	1.26E-02	Increased	2.089	20
Cell Morphology	shape change of neurons	1.26E-02	Increased	2.205	6

Table 3: Top associated biofunctions by IPA. Top significantly tumorigenesis-related biofunctions concerned with the ACSL4-induced transcriptome alteration in MCF-7 Tet-Off/ACSL4 cells. Only p-values under 0.01 calculated by right-tailed Fisher's Exact test were considered significant. IPA uses the activation z-score algorithm to make predictions. The z-score algorithm is designed to reduce the chance that random data will generate significant predictions.

Network	Score	Focus Molecules	Top Diseases and Functions	Molecules in Network
1	44	33	DNA Replication, Recombination, and Repair, Gene Expression, Cancer	CALCOCO1, CBX2, CBX5, CBX8, CHRNE, DIAPH2, ELF5, HIST1H3A (includes others), HIST1H4A (includes others), HIST2H2AA3/HIST2H2AA4, HIST2H2AC, HIST2H2BE (includes others), HIST2H3C (includes others), HIST3H2A, HOXD8, IL20, IL17R, IL17RC, KLF11, MSL3, MSMB, MT1G, NEK3, PARP10, RCC1, S100A7, SCML1, SHISA2, TEAD4, TFAP2C, TRANK1, TTC1, Vegf, WDR61, ZNF324B
2	43	32	Carbohydrate Metabolism, Small Molecule Biochemistry, Post-Translational Modification	A4GALT, ATL1, B4GALT1, B4GALT5, B4GALT6, B4GALT7, CDC42EP5, CMTM8, CYP4Z1, DSC2, EMCN, ERK1/2, ETV4, FAIM3, Galactosyltransferase beta 1, 4, GLIPR2, HS6ST2, KLF13, LINGO1, LRRN1, MMD, MUC5B, NDST1, NMU, OLFM1, PKP2, RAPGEF2, RTKN, RTN4R, RTN4RL2, SHC4, ST6GAL1, sulfotransferase, TP53TG1, ZNF217
3	35	28	Molecular Transport, Hereditary Disorder, Neurological Disease	ANO3, AP-3, AP3B2, AP3D1, ATP6V0A4, ATP6V0B, ATP6V1C2, CBR3, DOK3, EDARADD, EHF, ENO3, FBXO41, H+-exporting ATPase, H+-transporting two sector ATPase, KCND3, MIB2, MTORC1, NFIX, NFkB (complex), PDCD11, PGM1, PNKD, PRMT2, PRPH, RFTN1, S100, S100A1, S100P, SGCB, SGCG, TFEF, TMOD2, Vacuolar H+ ATPase, ZNF385A
4	31	26	Cellular Development, Embryonic Development, Developmental Disorder	ADAMTS9, ADCY, ADCY6, AGPAT9, Angiotensin II receptor type 1, BIK, C8orf4, CAPN8, DGAT2, EYA2, Fascin, FATE1, FSCN2, GABRB3, GGT5, GNAI1, HOXA5, INSIG2, IRS, Nr1h, NUCB1, p70 S6k, PADI2, PDE4D, PDE4DIP, Pkc(s), PODXL, PSCA, RGS6, SIX2, SLC1A1, SOCS, SP110, TPM2, TSH
5	31	26	Cardiovascular Disease, Cancer, Dermatological Diseases and Conditions	ABCC8, ABLIM1, ABLIM2, CCNG2, CRAT, DEAF1, DLX4, FOXO4, GATA6, GPX2, GUCY1A3, Hedgehog, Histone h4, ID3, KLF2, LMO2, Notch, NOTCH2, PI3K (family), PLEKHF1, PTCH1, PTCH2, QPCT, Ras, RCN1, Secretase gamma, SLC26A2, SMAD6, SMOOTH MUSCLE ACTIN, TAGLN, TCF, TNNT1, TOB2, ZC3H15
6	31	26	Carbohydrate Metabolism, Tissue Morphology, Ophthalmic Disease	ACAA2, Alpha catenin, BMP7, BRSK1, BSG, CBR4, CDH8, CHST11, CLDN23, CNKSR3, collagen, Collagen(s), CTGF, elastase, ERBB2, estrogen receptor, FAM134B, GJB3, HSD17B, HSD17B7, HSD17B8, HSD17B14, Integrin, KIFC3, MAP2K1/2, Mmp, MMP23B, PLEK2, PRR15L, RNF149, SOWAHC, SOX4, SYNPO, TSPAN4, ZNF703
7	29	25	Cell Morphology, Hair and Skin Development and Function, Organ Morphology	ACHE, Akt, ANTXR1, ARHGAP24, ASAH2, CHCHD2, chymotrypsin, COL18A1, COL6A2, Collagen type IV, Collagen type VI, CSF2RA, EPHB4, gelatinase, GPIIB-IIIA, GSTZ1, ITGA2, ITGB4, LAMB1, Laminin, Laminin1, MEX3B, MGLL, mir-29, MSR1, PID1, PPT1, PTTG1IP, RAP1GAP, SCARA3, SCAVENGER receptor CLASS A, STARD13, TACSTD2, TNFRSF21, Vla-4
8	29	25	Cell Morphology, Cellular Compromise, Lipid Metabolism	Alpha Actinin, Alpha tubulin, Ant, ARL2BP, ASCL2, ASIC3, Beta Tubulin, calpain, CLINT1, DCDC2, DHRS2, DMTN, DPYSL2, ESPN, F Actin, FMNL1, Focal adhesion kinase, GABARAPL1, MARCKS, Mucin, PACSIN1, SHROOM3, SLC25A4, SLC25A6, SNX33, Spectrin, STOM, Talin, TBC1D2B, TOMM20L, TPT1, TRDMT1, TSPO, VDAC1, WAS
9	29	25	Cancer, Dermatological Diseases and Conditions, Hematological Disease	60S ribosomal subunit, ANKRD13B, ATR, CCDC22, CCDC53, CCDC93, CKB, COL11A2, Collagen type II, CTSL, DNAJC27, Dynamin, E2F8, ENaC, ERRF1, FAM21A/FAM21C, HSP, Hsp27, Hsp70, HSPA8, let-7, mGluR, NXT2, OPTN, p85 (piK3r), RPL39, RPLP1, RRM2, SH3GL3, TM4SF1, TNRC6C, TRPC1, Ubiquitin, UCHL1, ZNF219
10	29	25	Endocrine System Development and Function, Small Molecule Biochemistry, Developmental Disorder	ACPP, ACSS1, ADRB, AGBL2, ATP9A, BOK, C8G, CA4, Cg, CHST8, Creb, DIO2, EPHB6, FAM198B, FAM214A, FSH, Igm, KHDRBS3, Lh, LIMCH1, MAMLD1, Mek, OGFR, ONECUT1, PLC, PTPN21, PTTG1, RAB33B, Raf, Rap1, RETSAT, SGSM2, SLCO4A1, TP53I11, YPEL3

Table 4: Gene networks of ACSL4-overexpressing cells. RNA-Seq data were analyzed for significantly regulated functions using IPA. The genes associated with each function network shown in the last column are significantly regulated in the ACSL4-overexpressing cells. Score: negative exponent of *p*-value calculated by a right-tailed Fisher's Exact test, which calculates the likelihood that network eligible molecules are found together by random chance alone.

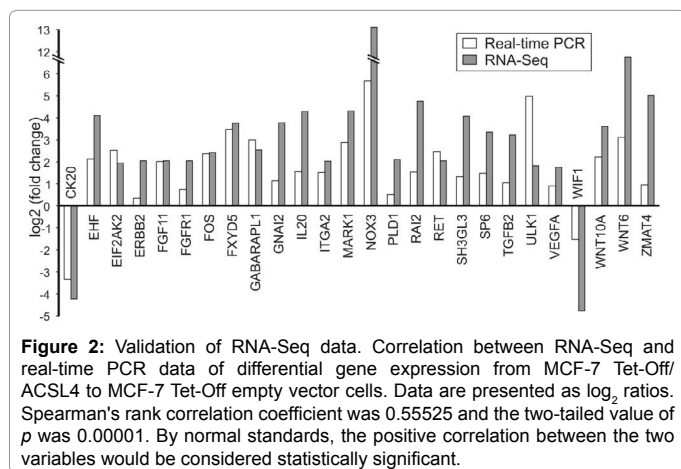


Figure 2: Validation of RNA-Seq data. Correlation between RNA-Seq and real-time PCR data of differential gene expression from MCF-7 Tet-Off/ACSL4 to MCF-7 Tet-Off empty vector cells. Data are presented as log₂ ratios. Spearman's rank correlation coefficient was 0.55525 and the two-tailed value of *p* was 0.00001. By normal standards, the positive correlation between the two variables would be considered statistically significant.

recombination, repair, gene expression and cancer showed the highest score. In particular, the finding that cellular development and embryogenesis are within the top ten biofunctions is interestingly in agreement with recent work showing the crucial role of ACSL4 pathways in embryo development in zebrafish [12] and *Drosophila* [14,24].

RNA-Seq data confirmed by analysis of gene expression changes by real-time RT-PCR

We further validated the gene expression changes found in RNA-Seq data and IPA by real-time RT-PCR in independent biologic repeats of samples from MCF-7 Tet-Off/ACSL4 and MCF-7 Tet-Off empty vector under the same conditions used for RNA-Seq analysis (relative mRNA expression levels are shown in (Figure 1). A comparison of fold changes between RNA-Seq and real-time RT-PCR for each gene is shown in Figure 2, which verifies that the real-time RT-PCR expression profiles were mostly in agreement with RNA-Seq data. Although there were small differences in the fold change values between the two methods of measurement, results were generally highly related (Spearman's rank correlation coefficient was 0.55525 and the two-tailed value of *p* was 0.00001) strongly supporting the reliability of our RNA-Seq analysis. We next focused our attention on categories that were relevant to this study, subgrouped these genes by function and measured an example of each of them (i.e. cytokines, transcription factors, growth factors, integrin family and cytoskeleton, Wnt signaling family, oncogenes, growth factor receptors and energy metabolism). Most of these genes have central roles in the biology of cancer cells regarding proliferation, migration and invasion. ACSL4 increased the

expression levels of interleukin 20 *IL20*, Ets homologous factor (*EHT*), SP6 transcription factor (Krueppel-like factor 14 or *SP6*), transforming growth factor beta 2 (*TGFβ2*), V-erb avian erythroblastic leukemia viral oncogene homologue 2 (*ERBB2*), vascular endothelial growth factor A (*VEFGA*), integrin alpha 2 (*ITGA2*), MAP/Microtubule affinity-regulating kinase 1 (*MARK1*), FXYP domain containing ion transport regulator 5 (*FXYP5*), ret proto-oncogene (*RET*), murine osteosarcoma viral oncogene homolog (*FOS*), fibroblast growth factor receptor 1 (*FGFR1*) and Wingless-Type MMTV Integration Site Family Member 6 (*WNT6*) and *WNT10A*. One of the genes showing a marked decrease after *ACSL4* expression was the WNT inhibitory factor 1 (*WIF1*). *IL20* has been demonstrated to be upregulated in muscle-invasive bladder cancer patients, while *EHT* and *SP6* are involved in differentiation and carcinogenesis. The *SP6* has also been proposed to contribute to the malignant phenotype of breast tumors. *TGFβ2*, *ERBB2*, *VEFGA*, *ITGA2*, *MARK1*, *FXYP5*, *RET* and *FOS* are involved in tumor progression as well. Other genes measured included the Unc-51-like autophagy-activating kinase 1 (*ULK1*) and the retinoic acid induced 2 (*RAI2*). In short, most of the genes confirmed to be upregulated here have well established roles in tumorigenesis. In addition, Table 5 shows the top small nuclear RNA and microRNA (miR) regulated by *ACSL4*. MicroRNAs play an important role in virtually all biological pathways and they may hence influence numerous cancer-relevant processes. *ACSL4* upregulates *miR-29a*, whose overexpression has been described to increase tube formation and migration in endothelial cultures. Mechanistically, *miR-29a* directly targets the phosphatase and tensin homolog (*PTEN*) in endothelial cells, leading to the activation of the AKT pathway [25]. *miR let-7*, an *ACSL4*-downregulated miR, represses cell proliferation pathways in human cells and has been described as a master regulator of cell proliferation pathways [26]. Overall, the RNA-Seq and IPA have identified genes that could potentially play important roles in the regulation of invasion and migration of breast tumor cells *in vivo*. We further studied enriched canonical pathways and analyzed them through IPA on the basis of RNA-Seq data. Eukaryotic translation initiation factor 2 (EIF2), protein ubiquitination, ribosomal protein S6 kinase 70kDa polypeptide 1 (p70S6K), mechanistic target of rapamycin (mTOR) and the signaling of molecular mechanisms of cancer are among the top canonical pathways triggered by *ACSL4* with the lowest *p*-values.

Signal transduction pathways triggered by *ACSL4* overexpression

In order to study the signaling pathway triggered by *ACSL4* on the basis of RNA-Seq bioinformatic studies, we next defined a functional protein signature of the *ACSL4* pathway by using RPPA, a high-throughput antibody-based technique developed for functional

Small nuclear RNA (some examples)	Gene Symbol	Location	Change
RNA, U12 small nuclear	<i>RNU12</i>	Nucleus	Upregulated
RNA, U4 small nuclear 1	<i>RNU4-1</i>	Nucleus	Upregulated
RNA, U4atac small nuclear (U12-dependent splicing)	<i>RNU4ATAC</i>	Nucleus	Upregulated
RNA, U5A small nuclear 1	<i>RNU5A-1</i>	unknown	Upregulated
RNA, U5D small nuclear 1	<i>RNU5D-1</i>	unknown	Upregulated
RNA, U5E small nuclear 1	<i>RNU5E-1</i>	unknown	Upregulated
small nucleolar RNA, H/ACA box 8	<i>SNORA4</i>	unknown	Downregulated
Micro RNA (some examples)	Gene Symbol	Location	Change
microRNA 29a	<i>miR-29</i>	Cytoplasm	Upregulated
microRNA 1290	<i>miR-1290</i>	Cytoplasm	Upregulated
microRNA 25	<i>miR-25</i>	Cytoplasm	Downregulated
microRNA let-7a-1	<i>let-7</i>	Cytoplasm	Downregulated
microRNA let-7d	<i>let-7</i>	Cytoplasm	Downregulated

Table 5: Top small nuclear RNA and microRNA regulated by *ACSL4*.

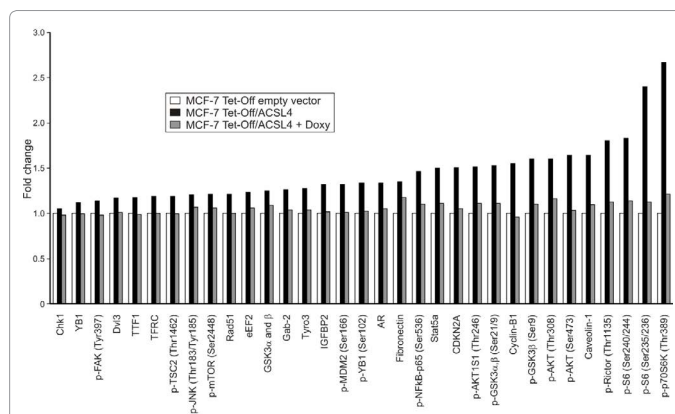


Figure 3: Identification of significantly upregulated protein expression or phosphorylation in *ACSL4*-overexpressing cells using RPPA. Proteins were extracted from MCF-7 Tet-Off empty vector, MCF-7 Tet-Off/*ACSL4* cells and doxycycline treated-MCF-7 Tet-Off/*ACSL4* (Doxy, 1 ug/ml, 48 h) cells, and were subjected to RPPA analysis. Data are presented as fold changes (only results with *p*-values under 0.05 are shown).

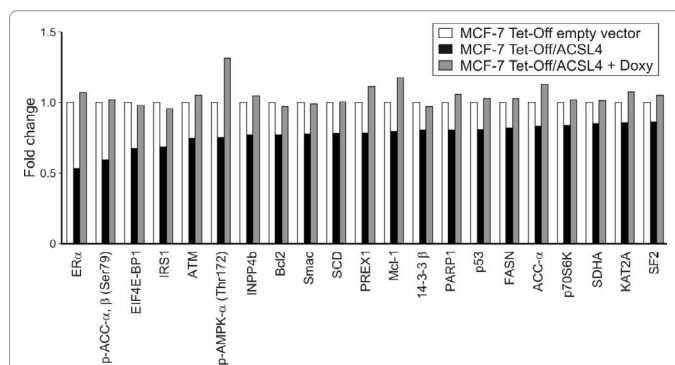


Figure 4: Identification of significantly downregulated protein expression or phosphorylation in *ACSL4*-overexpressing cells using RPPA. Proteins were extracted from MCF-7 Tet-Off empty vector, MCF-7 Tet-Off/*ACSL4* cells and doxycycline treated-MCF-7 Tet-Off/*ACSL4* (Doxy, 1 ug/ml, 48 h) cells, and were subjected to RPPA analysis. Data are presented as fold changes (only results with *p*-values under 0.05 are shown).

proteomic studies to measure phosphorylation states, as well as total levels of key signaling pathway intermediaries. This RPPA used 217 different antibodies directed to signaling proteins or directed to specific phosphorylated sites known to regulate protein signaling activity [22]. The analysis was performed on lysates derived from MCF-7 Tet-Off/*ACSL4*, MCF-7 Tet-Off empty vector and doxycycline-treated MCF-7 Tet-Off/*ACSL4* cells, the latter used to specifically override *ACSL4* expression. The pattern of protein expression and/or phosphorylation was remarkably different between MCF-7 Tet-Off/*ACSL4* and MCF-7 Tet-Off empty vector. Lysates from doxycycline-treated MCF-7 Tet-Off/*ACSL4* cells showed a pattern similar to that of MCF-7 Tet-Off empty vector, further supporting the role of *ACSL4* in the effects observed. Figures 3 and 4 show the proteins that exhibited a significant increase or decrease, respectively, in expression or phosphorylation status. *ACSL4* overexpression in MCF-7 breast cancer cells changed the pattern of expression or the pattern of phospho-dephosphorylation of about fifty proteins. These effects were reversed by doxycycline treatment, which confirms the specificity of the functional proteomic signature of *ACSL4*. We next performed a functional annotation analysis using the bioinformatic program DAVID on the basis of RPPA data. Figure 5 shows the DAVID scheme of pathways in cancer. *ACSL4* overexpression stimulated the dephosphorylation of two proteins and the phosphorylation of thirteen proteins, among which it markedly

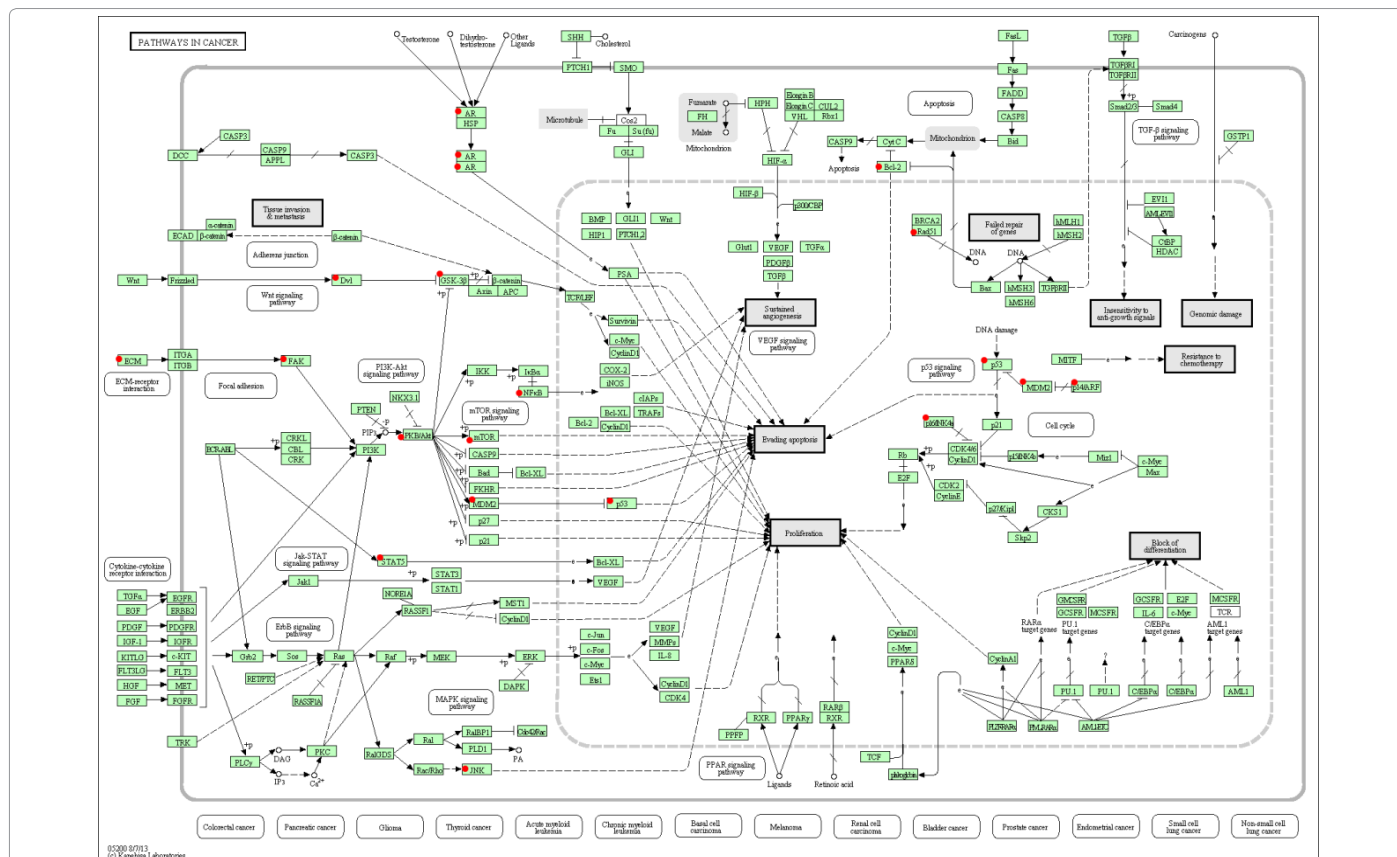


Figure 5: ACSL4 and pathways in cancer. Red marks highlight ACSL4-regulated genes in RPPA analysis. The pathway scheme was obtained from KEGG_PATHWAY database. Analysis was performed by DAVID bioinformatic tool.

stimulated the phosphorylation the mTOR pathway as previously described [22]. In accordance with the results mentioned above, ACSL4 overexpression also stimulates the expression of caveolin. Caveolin-1 is a ubiquitously expressed scaffolding protein which is enriched in caveolae –i.e. subtypes of lipid rafts– and which is involved in several cellular functions such as endocytosis, vesicular transport and signal transduction. Studies also revealed that caveolin-1 is an essential regulator of the invadopodia-mediated degradation of extracellular matrix, which indicates that caveolin-1 plays an essential role in cancer cell invasion [27]. Indeed, at least in breast cancer cell lines, caveolin-1 expression is predominantly observed in invasive cell lines and well correlated with invadopodia activity. These results correlate with those obtained in RNA-Seq, where cell movement showed the highest score (Table 3). Glycogen synthase kinase-3 alpha and beta (GSK3 α and GSK3 β), critical negative regulators of diverse signaling pathways, are two additional phosphoproteins whose levels exhibit an important increase in response to ACSL4 overexpression, and whose phosphorylation on Ser21 and Ser9, respectively, inhibits GSK3 activity. GSK3 has also been implicated in the negative regulation of FAK (focal adhesion kinase) activity [28]. As GSK3 α has been shown to inhibit the Wnt signaling pathway, the inhibition of GSK3 α activity by phosphorylation might suggest that Wnt signaling is part of the mechanism of action of ACSL4 overexpression. The aberrant regulation of the Wnt signaling pathway is a prevalent theme in cancer biology. From early observations that Wnt overexpression could lead to malignant transformation of mouse mammary tissue to the most recent genetic discoveries gleaned from tumor genome sequencing, the Wnt pathway continues to evolve as a central mechanism in cancer biology. Results from RNA-Seq also show that ACSL4 overexpression causes a

strong reduction in the expression of *WIF1*. The protein encoded by this gene inhibits Wnt proteins, which are extracellular signaling molecules playing a role in embryonic development. Mammary cancer is a prominent example involving the Wnt pathway, particularly cancers classified as basal-like or triple-negative [29,30] which characteristically involve the expression of Wnt receptor *FZD7* [31]. Accordingly, Yang et al. recently reported experiments in which knockdown of *FZD7*, in cell line models of triple-negative breast cancer, reduced the expression of Wnt target genes, inhibited tumorigenesis *in vitro* and greatly retarded the capacity of the MDA-MD-231 cell line to form tumors in mice [32]. These results suggest that Wnt ligands might drive certain breast cancers and are consistent with previous work from the Hynes laboratory [33]. In agreement with these data, ACSL4 overexpression increased the expression of *WNT6* and *WNT10A* (Figure 1). The *WNT6* gene is overexpressed in cervical cancer cell lines and strongly coexpressed with another family member, *WNT10A*, in a colorectal cancer cell line. *WNT6* overexpression may play a key role in carcinogenesis and is clustered with *WNT10A* in chromosome 2q35 region. The Wnt pathway is also implicated in the activation of mTORC1 through TSC1/2. In our studies, Wnt signaling inhibited GSK3 β , which normally phosphorylates and promotes TSC2 activity, and ACSL4 overexpression produced the stimulation of GSK3 on Ser9, which suggests that this mechanism of mTORC1 activation is also used by ACSL4 [22]. As mentioned above, ACSL4 overexpression increases the phosphorylation of GSK3 α and β , and a requirement for ACSL4 has recently been demonstrated in dorsoventral patterning of zebrafish embryo [12] and embryogenesis and neurogenesis in *Drosophila* [14,24]. These results show that ACSL4 works through the inhibition of AKT-dependent GSK3 activity by increasing its phosphorylation. And, given the interplay between morphogenic signals in developing

embryos, the interaction of these pathways might be expected in cancer. ACSL4 overexpression also stimulates the protein levels of growth factors and their receptors, such as the insulin-like growth factor binding protein (IGFBP2). Among genes involved in cell cycle control, ACSL4 decreases the level of the ataxia telangiectasia (*ATM*) gene, a kinase that regulates cell cycle checkpoints by phosphorylating multiple proteins including histone H2AX, CHK1 and CHK2 kinases and p53. *ATM* is activated through auto- or transphosphorylation on Ser1981 and/or Ser1893 in response to DNA damage, particularly the induction of DNA double-strand breaks. ACSL4 also produces a substantial increase in cyclin-B1, the oncogene E3 ubiquitin protein ligase (*MDM2*), the eukaryotic translation factor 4E binding protein 1 (*EEF2*) and the *GRB2*-associated binding protein 2 (*GAB2*). In the energy area, genes regulated are the acetyl-CoA-carboxylase alpha and beta (*ACC*) and the succinate dehydrogenase complex subunit a flavoprotein (*SDHA*), a part of the respiratory chain. *ACC* participate in fatty acid synthesis and oxidation and are phosphorylated by AMP-activated protein kinase (*AMPK*) on Ser79 to inhibit their activity. ACSL4 overexpression decreases the activity of *AMPK* and thus decreases the phosphorylation of *ACC*. Finally, another gene increased by ACSL4 is the disheveled segment polarity protein 3 (*DVL3*), a member of a multi-gene family which bears strong similarities with the *Drosophila* disheveled gene, which in turn encodes a cytoplasmic phosphoprotein that regulates cell proliferation. The idea of personalized medicine and molecular profiling for prognostic tests has led to a plethora of studies in the past 10 years, in search for genetic determinants of metastatic breast cancer. Such studies have identified gene sets, or “signatures”, whose expression in primary tumors is associated with higher risk of metastasis and poor disease outcome for the patients. Current views on cancer cell mutations hold that there are two different types: driver mutations, which are behind cancer growth because they give tumor cells a growth advantage, and passenger mutations, which are just along for the ride. It has been suggested that ACSL4 overexpression is led by a driver mutation [18,34]; however, as it is capable *per se* of changing cancer cell phenotypes, ACSL4 overexpression may be thought of as a backseat driver factor which generates changes in gene expression and signaling pathways toward a highly aggressive phenotype, and which acts in addition to passenger mutations when the driver gene is mutated. In summary, this study derives an ACSL4 overexpression gene and functional proteomic signature which might reveal important information about novel mediators of breast cancer cell aggressiveness. Here we report that ACSL4 overexpression can trigger several different mechanisms to regulate the aggressiveness of breast cancer cells, including the pathways stimulated by growth factors, nutrients, cytokines and changes in energy metabolism. The major findings of the present study are: (a) ACSL4 overexpression induces changes in genes associated with tumorigenesis-related biofunctions; (b) the four biofunctions with the highest activation z-scores are: cell movement, growth and proliferation, protein and cell assembly and organization; (c) the inhibition of ACSL4 expression completely abolishes the changes observed in protein expression and phosphorylation-dephosphorylation, which demonstrates the specificity of ACSL4 function; (d) since ACSL4 is *per se* capable of changing cancer cell phenotype, this protein overexpression may be thought of as a backseat driver factor which generates changes in gene expression and signaling pathways toward a highly aggressive phenotype; e) as ACSL4 has been related to colon and hepatocellular carcinoma, besides breast carcinoma, the present findings suggest novel mediators, specifically for combined pharmacological treatment toward tumor growth inhibition. Altogether, the present results open the possibility to use the inhibition of ACSL4 as a therapeutic tool in combination with agents targeting key molecular elements involved in breast cancer. In addition, ACSL4 could be used as a predictive marker that may provide the basis for patient therapy.

Acknowledgements

We thank Cristina Paz for her critical reading of the manuscript and María M. Rancez for providing language help and writing assistance. This work was supported by CONICET (PIP 2012-2014 - COD 11220110100485), Podesta; UBA (UBACYT 2011-2014 – 2002 0100100 849), Podesta.

References

1. Jemal A, Siegel R, Ward E, Murray T, Xu J, et al. (2007) Cancer statistics. *CA Cancer J Clin* 57: 43-66.
2. Monaco ME, Creighton CJ, Lee P, Zou X, Topham MK, et al. (2010) Expression of Long-chain Fatty Acyl-CoA Synthetase 4 in Breast and Prostate Cancers Is Associated with Sex Steroid Hormone Receptor Negativity. *Transl Oncol* 3: 91-98.
3. Maloberti PM, Duarte AB, Orlando UD, Pasqualini ME, Solano AR, et al. (2010) Functional interaction between acyl-CoA synthetase 4, lipoxygenases and cyclooxygenase-2 in the aggressive phenotype of breast cancer cells. *PLoS One* 5: e15540.
4. Orlando UD, Garona J, Ripoll GV, Maloberti PM, Solano AR, et al. (2012) The functional interaction between Acyl-CoA synthetase 4, 5-lipoxygenase and cyclooxygenase-2 controls tumor growth: a novel therapeutic target. *PLoS One* 7: e40794.
5. Wu X, Li Y, Wang J, Wen X, Marcus MT, et al. (2013) Long chain fatty Acyl-CoA synthetase 4 is a biomarker for and mediator of hormone resistance in human breast cancer. *PLoS One* 8: e77060.
6. Kang MJ, Fujino T, Sasano H, Minekura H, Yabuki N, et al. (1997) A novel arachidonate-preferring acyl-CoA synthetase is present in steroidogenic cells of the rat adrenal, ovary, and testis. *Proc Natl Acad Sci U S A* 94: 2880-2884.
7. Soupene E, Kuypers FA (2008) Mammalian long-chain acyl-CoA synthetases. *Exp Biol Med* (Maywood) 233: 507-521.
8. Watkins PA, Ellis JM (2012) Peroxisomal acyl-CoA synthetases. *Biochim Biophys Acta* 1822: 1411-1420.
9. Watkins PA (1997) Fatty acid activation. *Prog Lipid Res* 36: 55-83.
10. Li LO, Klett EL, Coleman RA (2010) Acyl-CoA synthesis, lipid metabolism and lipotoxicity. *Biochim Biophys Acta* 1801: 246-251.
11. Cao Y, Murphy KJ, McIntyre TM, Zimmerman GA, Prescott SM (2000) Expression of fatty acid-CoA ligase 4 during development and in brain. *FEBS Lett* 467: 263-267.
12. Miyares RL, Stein C, Renisch B, Anderson JL, Hammerschmidt M, et al. (2013) Long-chain Acyl-CoA synthetase 4A regulates Smad activity and dorsoventral patterning in the zebrafish embryo. *Dev Cell* 27: 635-647.
13. Maloberti P, Castilla R, Castillo F, Maciel FC, Mendez CF, et al. (2005) Silencing the expression of mitochondrial acyl-CoA thioesterase I and acyl-CoA synthetase 4 inhibits hormone-induced steroidogenesis. *FEBS J* 277: 1804-1814.
14. Y. Zhang Y, Gao Y, Zhao X, Wang Z (2011) *Drosophila* long-chain acyl-CoA synthetase acts like a gap gene in embryonic segmentation. *Dev Biol* 353: 259-265.
15. Gazou A, Riess A, Grasshoff U, Schaferhoff K, Bonin M, et al. (2013) Xq22.3-q23 deletion including ACSL4 in a patient with intellectual disability. *Am J Med Genet A* 161A: 860-864.
16. Modi HR, Basselin M, Taha AY, Li LO, Coleman RA, et al. (2013) Propylisopropylacetic acid (PIA), a constitutional isomer of valproic acid, uncompetitively inhibits arachidonic acid acylation by rat acyl-CoA synthetase 4: a potential drug for bipolar disorder. *Biochim Biophys Acta* 1831: 880-886.
17. Sung YK, Hwang SY, Park MK, Bae HI, Kim WH, et al. (2003) Fatty acid-CoA ligase 4 is overexpressed in human hepatocellular carcinoma. *Cancer Sci* 94: 421-424.
18. Cao Y, Dave KB, Doan TP and Prescott SM (2001) Fatty acid CoA ligase 4 is up-regulated in colon adenocarcinoma. *Cancer Res* 61: 8429-8434.
19. Jiang M, Huang O, Xie Z, Wu S, Zhang X, et al. (2014) A novel long non-coding RNA-ARA: adriamycin resistance-associated. *Biochem Pharmacol* 87: 254-283.
20. Database for Annotation, Visualization and Integrated Discovery (DAVID) <http://david.abcc.ncifcrf.gov>.
21. Ingenuity Pathways Analysis (IPA). <http://www.ingenuity.com>.

22. Orlando UD, Castillo AF, Dattilo MA, Solano AR, Maloberti PM, et al. (2015) Acyl-CoA synthetase-4, a new regulator of mTOR and a potential therapeutic target for enhanced estrogen receptor function in receptor-positive and -negative breast cancer. *Oncotarget* In press.
23. Pignatelli M, Serras F, Moya A, Guigo R, Corominas M (2009) CROC: finding chromosomal clusters in eukaryotic genomes. *Bioinformatics* 2512: 1552-1553.
24. Liu Z, Huang Y, Hu W, Huang S, Wang Q, et al. (2014) dAcsl, the *Drosophila* ortholog of acyl-CoA synthetase long-chain family member 3 and 4, inhibits synapse growth by attenuating bone morphogenetic protein signaling via endocytic recycling. *J Neurosci* 348: 2785-2796.
25. Endo Y, Toyama T, Takahashi S, Yoshimoto N, Iwasa M, et al. (2013) miR-1290 and its potential targets are associated with characteristics of estrogen receptor alpha-positive breast cancer. *Endocr Relat Cancer* 201: 91-102.
26. Johnson CD, Esquela-Kerscher A, Stefani G, Byrom M, Kelnar K, et al. (2007) The let-7 microRNA represses cell proliferation pathways in human cells. *Cancer Res* 6716: 7713-7722.
27. Yamaguchi H, Takeo Y, Yoshida S, Kouchi Z, Nakamura Y, et al. (2009) Lipid rafts and caveolin-1 are required for invadopodia formation and extracellular matrix degradation by human breast cancer cells. *Cancer Res* 6922: 8594-8602.
28. Golubovskaya VM (2010) Focal adhesion kinase as a cancer therapy target. *Anticancer Agents Med Chem* 1010: 735-741.
29. Geyer FC, Lacroix-Triki M, Savage K, Arnedos M, Lambros MB, et al. (2011) beta-Catenin pathway activation in breast cancer is associated with triple-negative phenotype but not with CTNNB1 mutation. *Mod Pathol* 242: 209-231.
30. Khramtsov AI, Khramtsova GF, Tretiakova M, Huo D, Olopade OI, et al. (2010) Wnt/beta-catenin pathway activation is enriched in basal-like breast cancers and predicts poor outcome. *Am J Pathol* 1766: 2911-2920.
31. Sorlie T, Tibshirani R, Parker J, Hastie T, Marron JS, et al. (2003) Repeated observation of breast tumor subtypes in independent gene expression data sets. *Proc Natl Acad Sci U S A* 10014: 8418-8423.
32. Yang L, Wu X, Wang Y, Zhang K, Wu J, et al. (2011) FZD7 has a critical role in cell proliferation in triple negative breast cancer. *Oncogene* 3043: 4437-4446.
33. Matsuda Y, Schlange T, Oakeley EJ, Boulay A, Hynes NE (2009) WNT signaling enhances breast cancer cell motility and blockade of the WNT pathway by sFRP1 suppresses MDA-MB-231 xenograft growth. *Breast Cancer Res* 113: R32.
34. Kaller M, Liffers ST, Oeljeklaus S, Kuhlmann K, Roh S, et al. (2011) Genome-wide characterization of miR-34a induced changes in protein and mRNA expression by a combined pulsed SILAC and micro-array analysis. *Mol Cell Proteomics*.

Citation: Castillo AF, Orlando UD, Lopez P, Solano AR, Maloberti PM, et al. (2015) Gene Expression Profile and Signaling Pathways in MCF-7 Breast Cancer Cells Mediated by Acyl-Coa Synthetase 4 Overexpression. *Transcriptomics* 3: 120. doi:[10.4172/2329-8936.1000120](https://doi.org/10.4172/2329-8936.1000120)

Submit your next manuscript and get advantages of OMICS Group submissions

Unique features:

- Increased global visibility of articles through worldwide distribution and indexing
- Showcasing recent research output in a timely and updated manner
- Special issues on the current trends of scientific research

Special features:

- 700 Open Access Journals
- 50,000 editorial team
- Rapid review process
- Quality and quick editorial, review and publication processing
- Indexing at PubMed (partial), Scopus, DOAJ, EBSCO, Index Copernicus and Google Scholar etc
- Sharing Option: Social Networking Enabled
- Authors, Reviewers and Editors rewarded with online Scientific Credits
- Better discount for your subsequent articles

Submit your manuscript at: <http://scholarscentral.com/>

Table S1. Detailed list of genes regulated by ACSL4 within the top three biofunctions by IPA.

Category	Diseases or Functions Annotation	p-value	Predicted Activation State	Activation z-score	Molecules	# Molecules
Cellular Movement	cell movement	3.97E-07	Increased	4.685	ABCC4, ACSL4, ADARB1, ADORA1, ANXA3, APOE, AREG/AREGB, ARHGAP24, ARHGAP8/PRR5-ARHGAP8, ASCL1, B4GALT1, BAI1, BMP7, BSG, BTC, CADPS2, CAMK1D, CCR1, CD82, CDKN2A, CEBPA, CELF3, CHRD, CHST10, CMTM8, CNTNAP2, COL18A1, CSF2RA, CTGF, CTNND2, CTSL, CXCL17, DCDC2, DDX58, DGCR6L, DIAPH2, DLX1, DLX2, DPYSL2, DYRK1B, EDN2, EFNA1, EFNB3, EGFL7, EHF, EPHB4, ERBB2, ERRF11, ETV4, ETV6, F2RL1, FGFR1, FGFR4, FHL1, FLT3LG, FOS, FOXO4, FURIN, GATA6, GCNT1, GGT5, GLIPR2, GNAI1, GPR173, GPR56, GRB7, GRN, GUCY1A3, HCAR2, HLA-G, HPGD, HSPA1A/HSPA1B, HSPB1, ID2, ID3, IGFBP5, IGSF8, IL20, IL24, IL6R, IL6ST, INSR, IRF6, IRF7, ITGA2, ITGB4, KLF2, LAMB1, let-7, MAFB, MAPK10, MARCKS, MARK1, MATK, MGLL, mir-29, MSR1, MT-ND1, MZF1, NCOA4, NDRG1, NDST1, NEURL, NFIX, NMU, NOD1, NOTCH2, NQO1, NTN1, NTRK3, ONECUT1, P2RX4, PARP9, PDCD4, PDE4D, PDE4DIP, PGR, PLD1, PODXL, PPP3CC, PREX1, PRMT2, PTGDR2, PTTG1, QPCT, RAP1GAP, RAPGEF1, RAPGEF2, REPS2, RET, RHOBTB2, RHO, RNF144A, RPS6KA1, S100A1, S100A12, S100A7, S100A8, S100A9, S100P, SCARB1, SCPEP1, SDC1, SH3PXD2B, SHC4, SKI, SLPI, SOCS2, SORBS3, SORD, SPHK1, SPRY4, ST6GAL1, STARD13, SYK, TACSTD2, TAZ, TENC1, TERC, TFAP2C, TGFB111, TGFB2, THBD, THRA, TM4SF1, TMSB10/TMSB4X, TNFRSF11B, TNFRSF21, TNFSF9, TNS1, TP73, TPT1, TRPC1, TSPO, VASH1, VAV1, VIPR1, VIPR2, WAS, WNT10B, ZNF217, ZSCAN1	182
Cellular Movement	migration of cells	4.65E-07	Increased	4.677	ABCC4, ACSL4, ADARB1, ADORA1, ANXA3, APOE, AREG/AREGB, ARHGAP24, ARHGAP8/PRR5-ARHGAP8, ASCL1, B4GALT1, BAI1, BMP7, BSG, BTC, CADPS2, CAMK1D, CCR1, CD82, CDKN2A, CEBPA, CHRD, CHST10, CMTM8, CNTNAP2, COL18A1, CSF2RA, CTGF, CTSL, CXCL17, DCDC2, DDX58, DGCR6L, DIAPH2, DLX1, DLX2, DPYSL2, DYRK1B, EDN2, EFNA1, EFNB3, EGFL7, EHF, EPHB4, ERBB2, ERRF11, ETV4, ETV6, F2RL1, FGFR1, FHL1, FLT3LG, FOXO4, FURIN, GATA6, GCNT1, GGT5, GLIPR2, GNAI1, GPR173, GPR56, GRB7, GRN, GUCY1A3, HCAR2, HLA-G, HPGD, HSPA1A/HSPA1B, HSPB1, ID2, ID3, IGFBP5, IGSF8, IL20, IL24, IL6R, IL6ST, INSR, IRF6, IRF7, ITGA2, ITGB4, KLF2, LAMB1, let-7, MAFB, MAPK10, MARCKS, MARK1, MATK, MGLL, mir-29, MSR1, MT-ND1, MZF1, NDRG1, NDST1, NFIX, NMU, NOD1, NOTCH2, NQO1, NTN1, NTRK3, ONECUT1, P2RX4, PARP9, PDCD4, PDE4D, PDE4DIP, PGR, PLD1, PODXL, PREX1, PRMT2, PTGDR2, PTTG1, QPCT, RAP1GAP, RAPGEF1, RAPGEF2, REPS2, RET, RHOBTB2, RHO, RNF144A, S100A12, S100A7, S100A8, S100A9, S100P, SCARB1, SCPEP1, SDC1, SH3PXD2B, SHC4, SLPI, SORBS3, SPHK1, SPRY4, ST6GAL1, SYK, TACSTD2, TAZ, TENC1, TERC, TFAP2C, TGFB111, TGFB2, THBD, TM4SF1, TMSB10/TMSB4X, TNFRSF11B, TNFRSF21, TNFSF9,	166

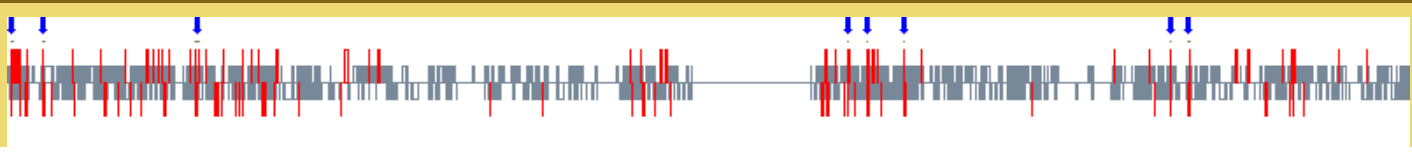

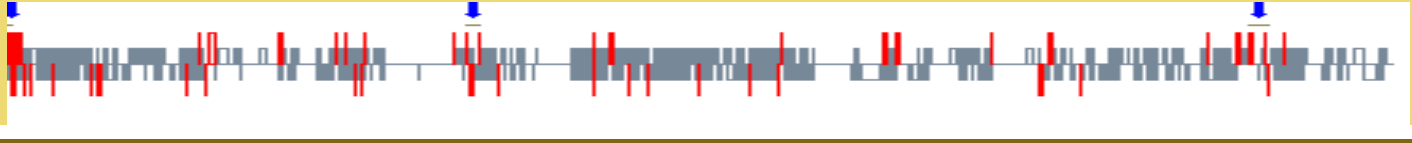
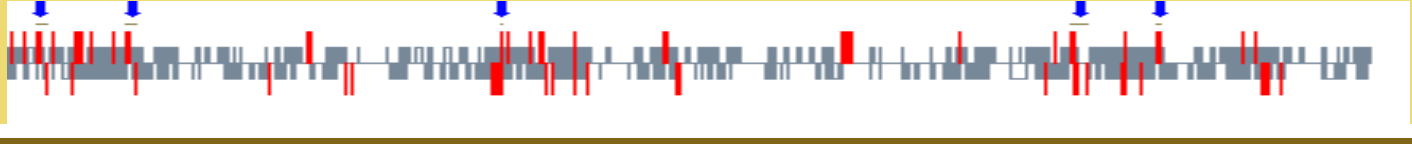
Figure S1. Chromosome distribution patterns of differentially expressed genes and gene clusters of ACSL4-overexpressing cells.

The analysis was performed with the CROC program (<http://metagenomics.uv.es/CROC>) and results were corrected by the Benjamini & Hochberg multiple test correction method. The minimum number of genes per cluster was 3 and the reference type of statistical analysis was by chromosome.

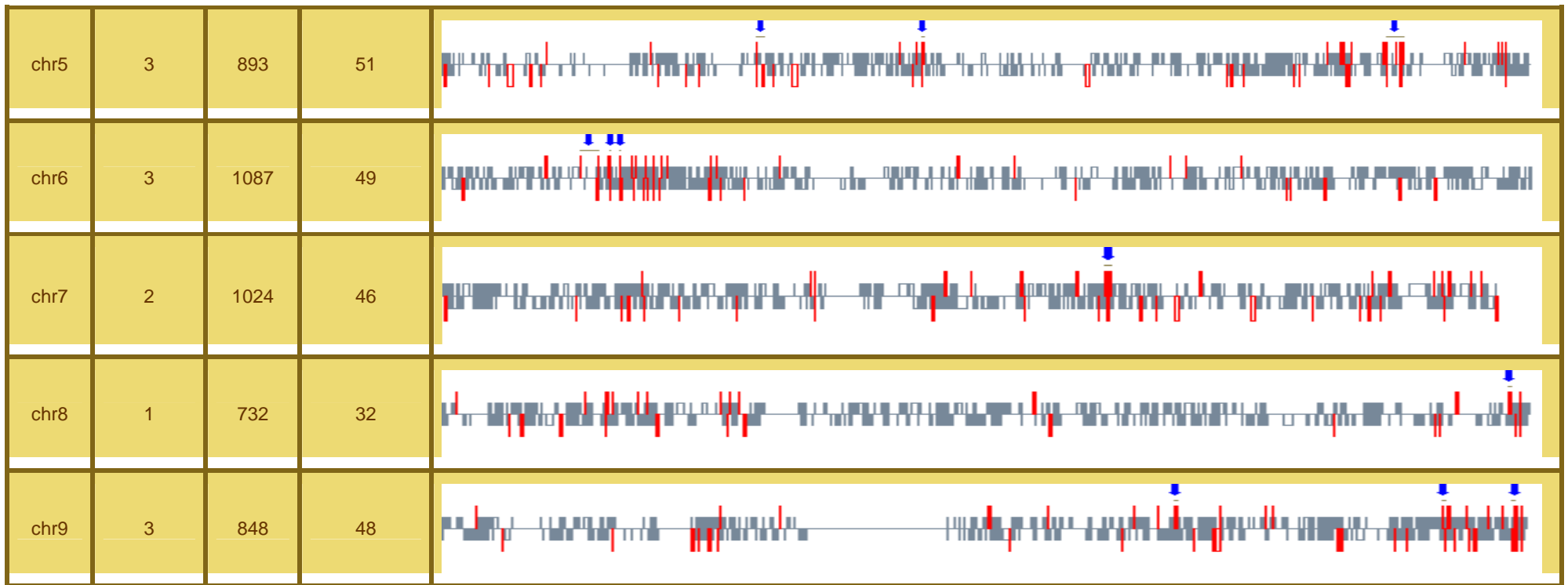
>> **Stats**

User genes found in reference genome	960
Number of Unknown genes	1183
Number of clusters found	52
Total number of genes in clusters	508
Number of user genes in clusters	181

>> **Chromosomes**

Chrom	Clusters	Genes	In user set	
chr1	8	2107	119	
chr10	1	812	29	
chr11	3	1364	53	
chr12	5	1056	58	

chr15	1	655	31	
chr16	2	900	27	
chr17	4	1230	65	
chr19	2	1453	58	
chr2	3	1356	78	
chr20	4	577	28	
chr22	1	538	29	
chr3	3	1096	43	
chr4	3	777	48	



>> **Clusters**

Chr	Begin	End	p-value	Genes	Plot
chr1	850393	939718	5.20e-03	SAMD11 C1orf170 ISG15	
chr1	6231988	6502158	5.20e-03	PLEKHG5 GPR153 ESPN	

chr1	33132996	33733660	5.20e-03	TMEM54 ADC TRIM62 ZSCAN20	
chr1	148051453	148126090	1.92e-07	HIST2H3D HIST2H2AA4 HIST2H3C HIST2H2AC HIST2H2AA3 HIST2H2AB HIST2H2BE HIST2H3A	
chr1	151597384	151698113	2.97e-04	S100A7 S100A12 S100A8 S100A9	
chr1	158017515	158179898	5.20e-03	DUSP23 CCDC19 IGSF9	
chr1	205105821	205161822	5.20e-03	FAIM3 IL20 IL24	
chr1	208028391	208482302	5.20e-03	C1orf133 SERTAD4 IRF6	

chr10	105148174	105340116	1.30e-03	NEURL PDCD11 CALHM2	
chr11	301317	480579	1.74e-03	IFITM1 IFITM3 PTDSS2	
chr11	44572789	45789459	1.74e-03	SYT13 TP53I11 SLC35C1 CD82	
chr11	120828251	122437242	1.74e-03	SORL1 C11orf63 HSPA8	
chr12	2974194	3809442	4.71e-03	TEAD4 TSPAN9 PARP11	
chr12	11694329	12565299	4.71e-03	ETV6 MANSC1 DUSP16	
chr12	47975251	48031549	4.71e-03	DNAJC22 PRPH C1QL4	

chr12	103375320	105056561	4.71e-03	CHST11 SLC41A2 NUAK1	
chr12	111829228	111932669	4.71e-03	OAS2 OAS1 OAS3	
chr15	86221173	86999763	2.96e-03	NTRK3 DET1 ISG20	
chr16	55702156	55875953	7.80e-04	ARL2BP CPNE2 PLLP	
chr16	56104157	56389656	7.80e-04	CCDC102A GPR56 KIFC3	
chr17	39741622	39936264	4.24e-03	RUNDC3A GRN GPATCH8	
chr17	40655275	40915633	4.24e-03	ARHGAP27 FMNL1 PLEKHM1	
chr17	45401832	45557322	4.24e-03	SAMD14 DLX4 PDK2	

chr17	70979582	71134156	4.24e-03	KIAA0195 CASKIN2 MYO15B	
chr19	1988741	2180788	1.89e-03	DOT1L MKNK2 AP3D1	
chr19	63144107	63332682	1.89e-03	ZSCAN18 ZNF256 ZNF329 ZSCAN1	
chr2	6907435	8740477	5.42e-03	RNF144A CMPK2 ID2	
chr2	19960232	20288109	5.42e-03	MATN3 TTC32 SDC1	
chr2	220117694	220214691	3.11e-04	TMEM198 SLC4A3 INHA OBSL1	
chr20	38749936	39420917	3.15e-03	LPIN3 ZHX3 MAFB	

chr20	42676612	42872326	3.15e-03	KCNK15 PKIG RIMS4	
chr20	45040678	46877804	3.15e-03	EYA2 ZMYND8 PREX1	
chr20	54638008	55416305	3.15e-03	RBM38 TFAP2C BMP7	
chr22	41226621	41889018	4.27e-03	TSPO SERHL SERHL2 A4GALT BIK	
chr3	31678571	32386460	1.77e-03	OSBPL10 ZNF860 CMTM8	
chr3	123729904	123930131	1.77e-03	PARP15 PARP14 PARP9	
chr3	128867472	129609789	1.77e-03	ABTB1 MGLL EEFSEC	
chr4	75529927	76708670	3.93e-04	BTC AREGB AREG C4orf26	

chr4	77576230	78325283	6.51e-03	ANKRD56 SHROOM3 CCNG2	
chr4	89402774	89646049	6.51e-03	PPM1K HERC6 HERC5	
chr5	52321056	53642030	5.23e-03	ARL15 MOCS2 ITGA2	
chr5	79819699	80207434	5.23e-03	ANKRD34B MSH3 FAM151B	
chr5	157091027	159788263	2.92e-04	THG1L LSM11 CLINT1 PTTG1 PWWP2A SLU7 CCNJL TTC1 UBLCP1	
chr6	21702745	24466098	2.65e-03	DCDC2 SOX4 KAAG1	
chr6	26324473	26393706	1.16e-04	HIST1H1D HIST1H2BI HIST1H2BG HIST1H2BH HIST1H3F HIST1H3G HIST1H4H	

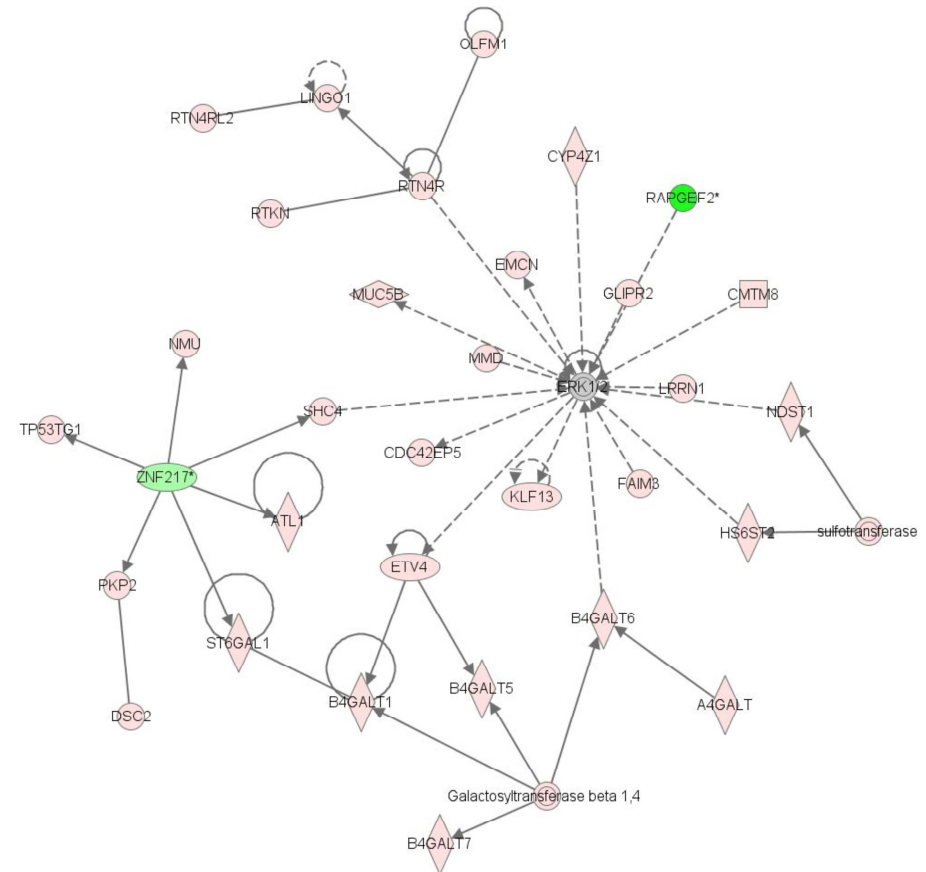
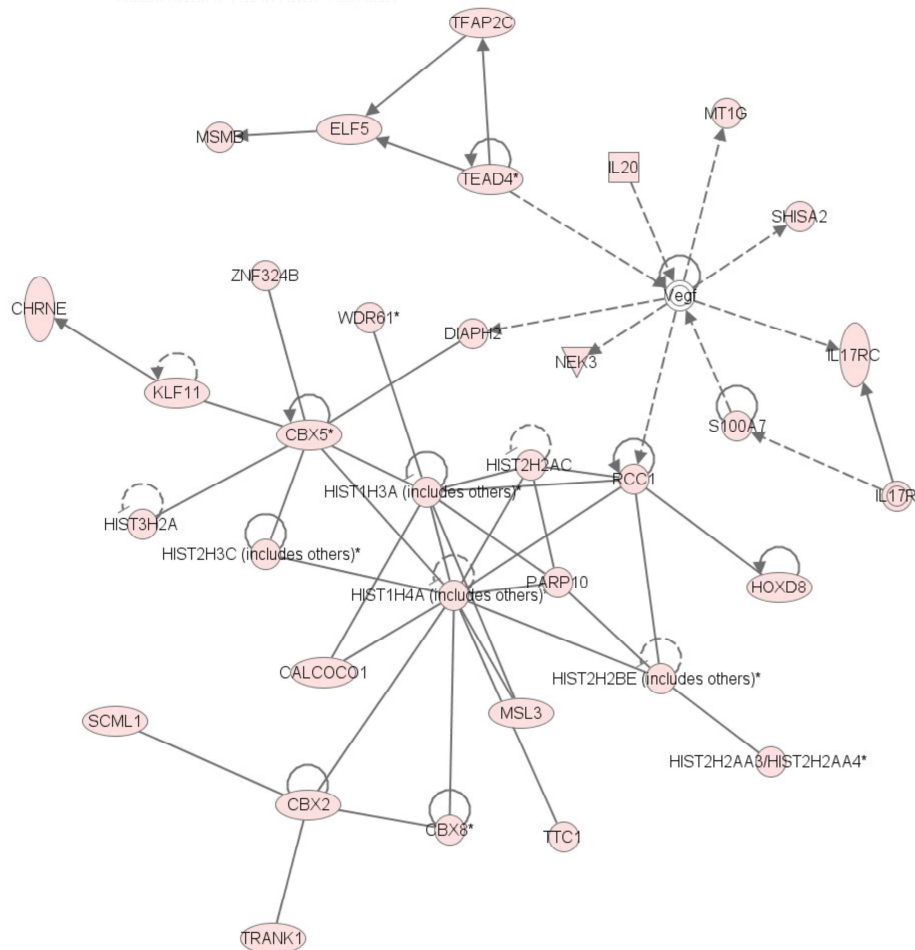
chr6	27883286	27907284	1.16e-04	HIST1H2AJ HIST1H4K HIST1H2BL HIST1H4J	
chr7	99743445	99913597	2.62e-03	TSC22D4 MEPCE AC005071.2 PILRA	
chr7	100239022	100519578	2.62e-03	TRIM56 ACHE MUC3A EPHB4	
chr8	143542562	143813856	2.36e-03	BAI1 PSCA C8orf55	
chr9	94778360	94915207	5.08e-03	FGD3 SUSD3 C9orf89	
chr9	129414504	129537384	5.08e-03	TOR2A STXBP1 PTRH1	
chr9	138456031	138701630	5.08e-03	EGFL7 SEC16A AGPAT2	

Figure S2. Top ranked networks identified by IPA from ACSL4-overexpressing cells.

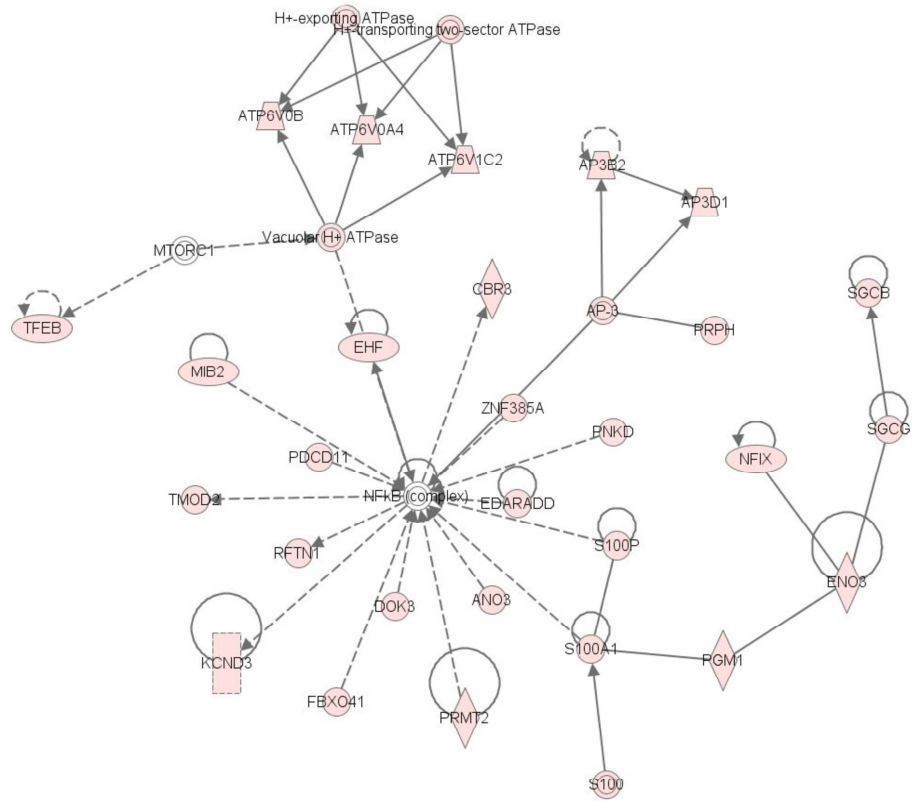
Networks are displayed graphically as nodes (genes/gene products) and edges (biological relationships between the nodes). Intensity of the node color indicates the degree of regulation (red: upregulation, green: downregulation, white: not differentially expressed but related to this network).

A: Network for DNA Replication, Recombination, and Repair, Gene Expression, Cancer (score: 44).

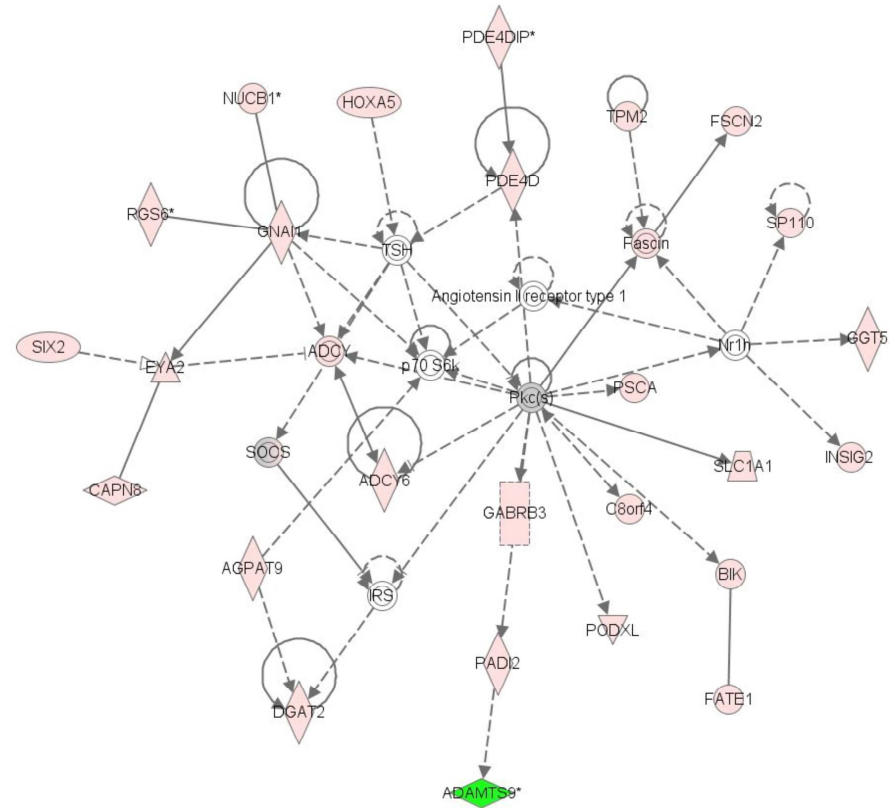
B: Network for Carbohydrate Metabolism, Small Molecule Biochemistry, Post-Translational Modification (score: 43).



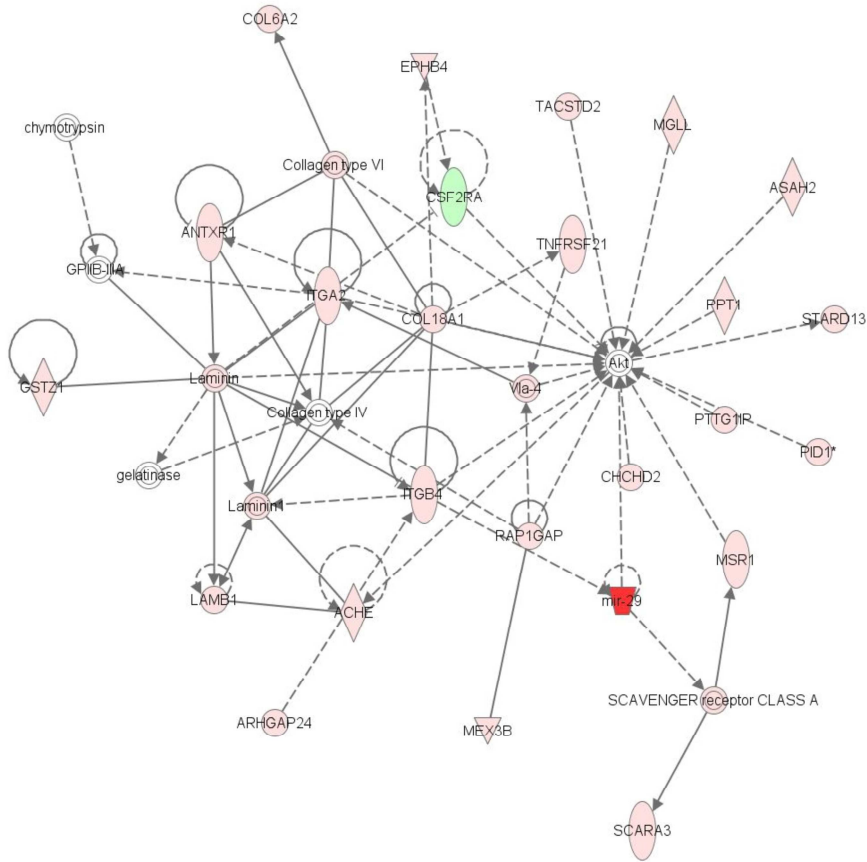
C: Network for Molecular Transport, Hereditary Disorder, Neurological Disease (score: 35).



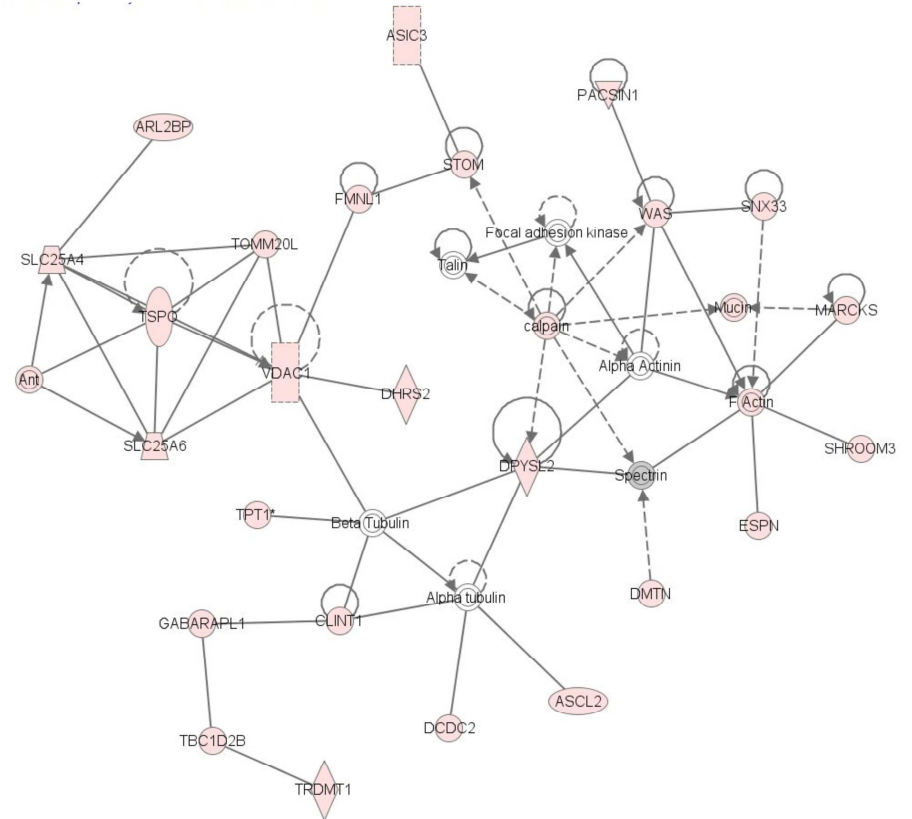
D: Network for Cellular Development, Embryonic Development, Developmental Disorder (score: 31).



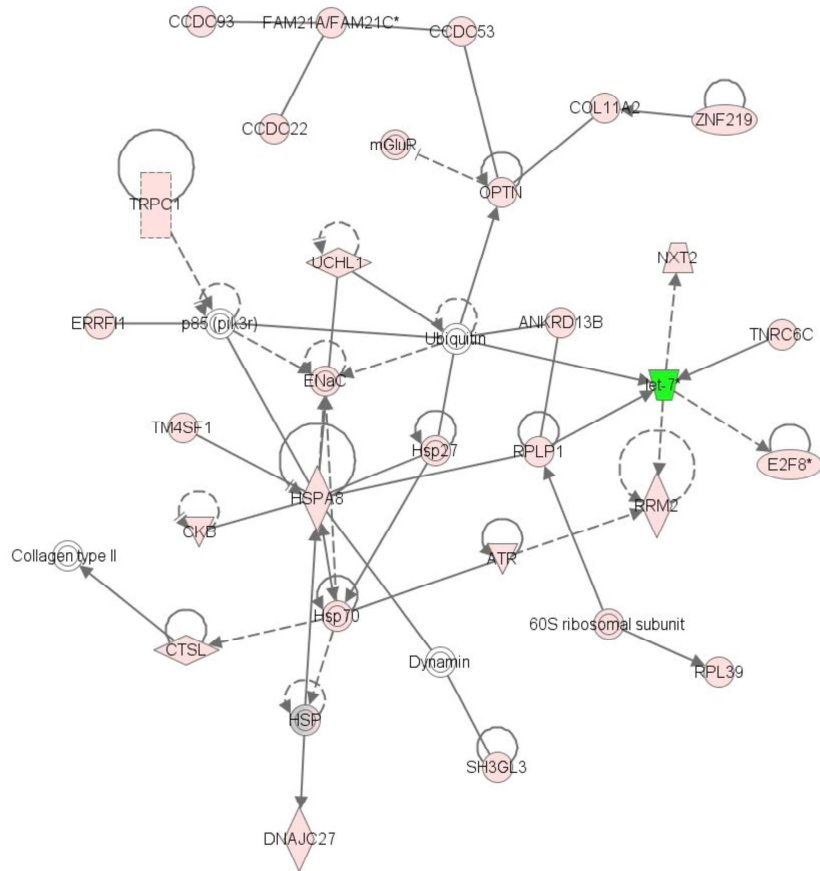
G: Network for Cell Morphology, Hair and Skin Development and Function, Organ Morphology (score: 29).



H: Network for Cell Morphology, Cellular Compromise, Lipid Metabolism (score: 29).



I: Network for Cancer, Dermatological Diseases and Conditions, Hematological Disease (score: 29).



J: Network for Endocrine System Development and Function, Small Molecule Biochemistry, Developmental Disorder (score: 29).

